A Novel Approach for the Restoration of AFM Images that were Produced Using the Impulse Response Technique at Different Scanning Speeds

AHMED AHTAIBA , ABDULWANIS ABDULHADI , H.M. AMREIZ AND OTMAN IMRAYED
Electrical and Electronic Engineering Department
Sirte University
Sirte
LIBYA
Amaa_1973@yahoo.com

Abstract: - The atomic force microscope is a very useful tool for use in biology and in nano-technology, since it can be used to measure a variety of objects such as cells and nano-particles in a variety of different environments. However, the images produced by the AFM are distorted and do not accurately represent the true shape of the measured cells or particles, even though many researchers do not take this fact into account. In this paper we determine the impulse response of AFM using experimental results gathered from measuring the cylindrical sample via AFM. Once the AFM impulse response is estimated, the Lucy- Richardson algorithm is used to calculate the deconvolution between the resultant AFM impulse response and the blurred AFM image. This produces a more accurate AFM image. Also in this paper, we compare raw experimental AFM images with the Restored AFM images quantitively and the proposed algorithm is shown to provide superior performance.

Key-Words: - AFM, Impulse response, deconvolution, image restoration, scanning speed, pillar sample.

1 Introduction

All atomic force microscope (AFM) images suffer from distortions, which are produced by the interaction between the measured sample and the AFM impulse response. If the impulse response of the AFM is known, the distorted image can be processed and the original surface form 'restored', typically by deconvolution approaches. This restored image gives a better representation of the real 2D surface of the measured sample than the original distorted image.

The problem of reconstructing the actual surface topography of an AFM sample has been investigated by many researchers. The AFM image was restored by Pingali and Jain using mathematical morphological operators [1]. The AFM tip shape was reconstructed from AFM images of known samples by Keller and Franke, who used the reconstructed AFM tip for the restoration of the AFM images [2]. Blind tip reconstruction was developed by Villarrubia,

which is also based on the mathematical morphology [3]. Dongmo used this algorithm for reconstructing a stylus profilometer tip, then a comparison was carried out between the reconstructed tip shape and its Scanning Electron Microscope (SEM) image [4]. Subsequently Todd showed that noise in the AFM image causes a distortion in the tip estimation and proposed an approach to improve the algorithm [5]. Recently Tranchida has taken the effects of operating parameters (for instance, sampling intervals and instrumental noise) into consideration in the practical use of the algorithm [6]. After that they introduced guidelines and the appropriate experimental conditions that are relevant to the blind estimation algorithm.

In this paper we estimate the impulse response of the AFM using experimental results that have been gathered from measuring a cylindrical pillar sample via AFM. Once the AFM impulse response is estimated, a

Ahmed Ahtaiba, Abdulwanis Abdulhadi,
H. M. Amreiz, Otman Imrayed

deconvolution process may be used between the resultant AFM impulse response and the blurred raw AFM image. This produces a more accurate AFM image.

2 AFM impulse response estimation using a cylindrical pillar sample

Contact mode AFM was used to measure the standard sample HS-100MG with known dimensions, that is constructed from silicon and which consists of a 2D array of small cylindrical columns. After this AFM measurement a single pillar was selected from the image.

A threshold was chosen for determining the area of the top of the column within the AFM image, which is approximately an entire circle, as is shown in Fig.1(a). The outer boundary of the pillar was determined using the Canny edge detection algorithm and the result of this edge detection is depicted in Fig.1(b). Then the outer boundary of the circle was expanded in order to estimate the associated tip distortion data that were available around the periphery of the column, as illustrated in Fig.1(c). The expansion in size is chosen to be in the range of $1.2d$ and $2d$ approximately, where d is the diameter of the cylinder. Next, we applied Breshamn's line algorithm to move the tip data that were located around the outer boundary of the cylinder radially inwards towards the centre of the previously removed cylinder and Fig.1(d) shows the result, which represents the 3-D estimated AFM impule response shape using this proposed algorithm.

The widely used Lucy- Richardson algorithm uses the priori information of non-negativity and flux conservation. It produces a AFM restored image through an iterative method. The idea is to imagine that the ideal AFM image is convoluted with the impulse response of the AFM. The Lucy-Richardson Algorithm maximizes the likelihood function of the image, which is modelled with Poisson statistics [7]; [8]. The estimated image for the first time usually is the blurred image. The Lucy-Richardson algorithm uses such an iterative algorithm [9].

$$f_{k+1}(x,y) = f_k(x,y) \frac{g(x,y)*h(-x,-y)}{[h(x,y)*f_k(x,y)]*h(-x,-y)} \quad (1)$$

Where $g(x,y)$ is the blurred AFM image, $h(-x,-y)$ is the transpose of the impulse response of the system, $f_k(x,y)$ is the previous estimate of the AFM image, $h(x,y)$ is the impulse response of the AFM system, and $f_{k+1}(x,y)$ is the current estimate of the AFM image.
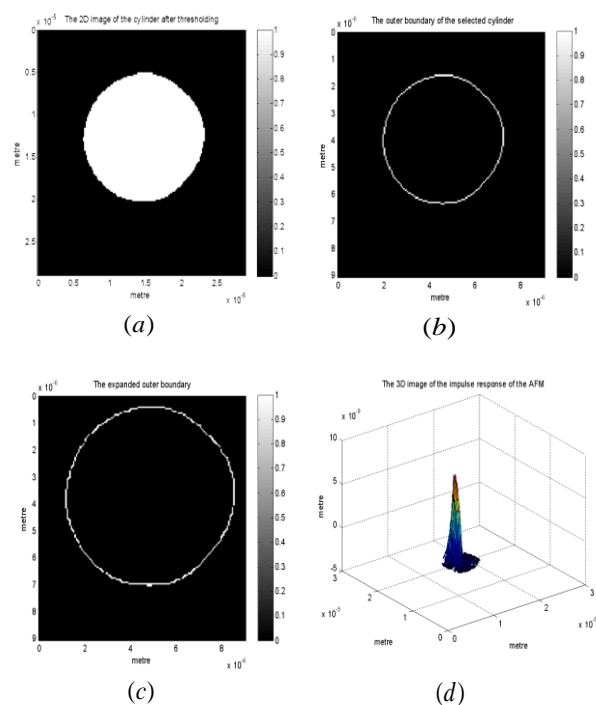

(a)   (b)

(c)   (d)

Fig.1 Illustrates the steps of the experimental procedure for estimating the impulse response of the AFM: (a) thresholding a standard sample that contains a cylinder with known dimensions, (b) determining the location of the cylinder in the image by defining the outer boundary; (c) determining the outer boundary and then expanding the outer boundary for removing the pixels that belong to the cylinder from the image; (d) extracting the impulse response of the AFM.

3 Experimental Results

3.1 Restoration of AFM images at a scanning speed of 1 Hz

In this section, two real samples were measured using contact mode AFM at a scanning speed of 1 Hz. These samples were as follows; a real sample that contains an array of raised cylindrical pillars, and a real sample that contains a grid of raised square pillars. At this scanning speed the same steps that were explained above, and which are shown in Fig.1,

Ahmed Ahtaiba, Abdulwanis Abdulhadi,
H. M. Amreiz, Otman Imrayed

were implemented. Once the impulse response was obtained at this scanning speed, a Lucy-Richardson deconvolution process was carried out between the resultant impulse response of the AFM and the blurred raw AFM image (that had been measured at the same AFM scanning speed as that which was used to derive the impulse response). As a result for the AFM image of a real sample that contains an array of cylindrical pillars, it can be seen that, after applying the Lucy- Richardson deconvolution procedure, the restored AFM image is qualitatively improved in terms of its fidelity, as is illustrated in Fig.2(c).

Table 1 shows numerical information results at a scanning speed of 1 Hz in the AFM image and the reconstructed image that are illustrated in Fig.2(a) and Fig.2(c), respectively. In this table, the measurement results are taken from the first row of pillars in the AFM image and compared with the results in the corresponding row in the restored AFM image. The height (H1) of a point that lies at a position (X = $2.647\mu m$, Y=$2.441\mu m$), which is approximately the centre of the first pillar P(1,1) in the first row of pillars within the AFM image is equal to 91.38 nm. Whereas the corresponding height (H2) in the restored image is 91.68 nm. The difference between the two heights H1, H2 is 0.3 nm. This corresponds to a percentage of difference (D%) equal to 0.327%.

For the second pillar P(1,2) that lies at a position (X=$7.617\ \mu m$, Y = $2.441\ \mu m$) in the first row of the AFM image, the height (H1) is 88.59 nm. The corresponding height in the restored image is 88.89 nm. The difference between H1 and H2 is 0.3 nm, which represents a percentage of difference equal to 0.337%.

In the third pillar P(1,3) within the same row in the AFM image, the height (H1) that lies at a position (X=$12.62\ \mu m$, Y = $2.441\ \mu m$) is 86.24 nm. The corresponding height (H2) in the restored image is 86.52 nm. The difference between H1 and H2 is 0.28 nm,which corresponds to a percentage difference of 0.323%.

It can be seen that the small percentage is 0.323% when the differences between H1 and

H2 at a scanning speed of 1 Hz are compared quantitatively.

Pillar position	P(1,1)	P(1,2)	P(1,3)
X[μm]	2.647	7.617	12.62
Y[μm]	2.441	2.441	2.441
H1[nm]	91.38	88.59	86.24
H2[nm]	91.68	88.89	86.52
D[nm]	0.3	0.3	0.28
D%	0.327%	0.337%	0.323%

Table 1 a comparison of quantitative values of the first row of pillars in the AFM image (Fig. 2(a)) with the values of the corresponding row in the restored image (Fig. 2(c))
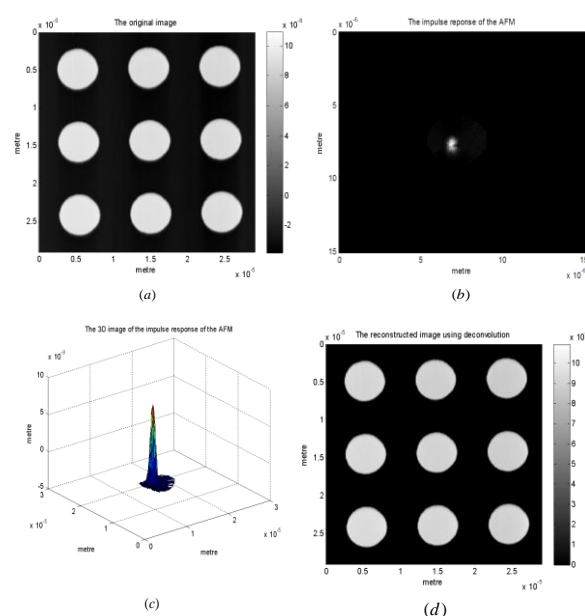

(a)   (b)

(c)   (d)

Fig.2 depicts a comparison between the raw experimental AFM image and the restored AFM image that was produced using the proposed technique at a scanning speed of 1 Hz: (a) the image of the real sample that contains cylindrical pillars measured by an AFM tip; (b) the 2D view of the impulse response of the AFM; (c) the 3D view of the impulse response of the AFM; (d) the restored AFM image after applying a Lucy-Richardson deconvolution method between the AFM image and the estimated impulse response of the AFM.

Restoration of subsequent images produced by the AFM can be carried out by performing a Lucy-Richardson deconvolution process between the raw AFM image that is acquired by the instrument and the AFM's impulse response

that may be found as detailed in previous section and which is shown in Fig.1.

Fig.s 3(a) and 3(b) compare the raw AFM topographical image of an array of raised square pillars as measured at a scanning speed of 1 Hz with the restored AFM image after applying the Lucy-Richardson deconvolution method respectively. This comparison indicates that the Lucy-Richardson deconvolution approach works properly and the restored image is improved in terms of its fidelity, as is depicted in Fig.3(b).
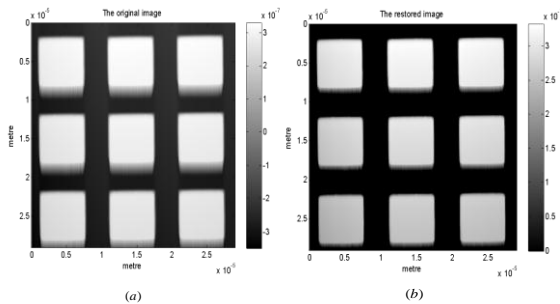

(a)   (b)

Fig.3 Illustrates a comparison between the raw experimental AFM image and the restored AFM image that was produced using the proposed technique at a scanning speed of 1 Hz : (a) The image of the real sample that contains square pillars measured by an AFM tip; (b) The restored AFM image after applying a Lucy-Richardson deconvolution between the AFM image and the estimated AFM impulse response.

3.2 Restoration of AFM images at a scanning speed of 2 Hz

In this section, the same real samples that have been previously measured at 1 Hz are used. However, in the following section the experimental images of the aforementioned real samples were produced by the AFM measuring at a scanning speed of 2 Hz. Fig.s 4(a), and 5(a) show the experimental images of a real sample that contains an array of raised cylindrical pillars, and a grid of raised square pillars, respectively. Restoration of experimental images that are subsequently produced by the AFM at a scanning speed of 2 Hz can be carried out by performing a Lucy-Richardson deconvolution process between the raw AFM image that is acquired directly from the instrument and the approximated AFM impulse response that was produced as described in section 2 and which is illustrated in Fig.4(c). As a result, it can be seen that the restored images which are shown in Fig.s 4(d), and 5 (b), respectively, are qualitatively improved in

terms of their fidelity when they are compared with the corresponding raw experimental AFM images.

Table 2 indicates quantitative values that were taken from the first row of pillars in the AFM image, which is depicted in Fig.4(a) and compared with the corresponding values in the restored image that is shown in Fig.4(d). The AFM image was measured at a scanning speed of 2 Hz. The height (H1) of the pillar P(1,1) that lies at a position (X = 2.647 μm, Y = 2.441 μm) is 91.59 nm. The height (H2), which is the corresponding height in the restored image is 92.14 nm. The difference (D) between H1 and H2 is 0.55 nm that represents a percentage difference of 0.596%.

The height (H1) of the second pillar P(1,2) that lies at a position (X = 7.617 μm, Y = 2.441 μm) is 94.2 nm. The corresponding height (H2) in the restored image is 94.76 nm. The difference (D) between H1 and H2 for P(1,2) is 0.56 nm, which represents a percentage difference of 0.590%.

For the pillar P(1,3), the height (H1) that lies at a position (X = 12.62 μm, Y = 2.441 μm) is 86.65 nm. The corresponding height (H2) in the restored image is 87.17 nm. The difference between H1 and H2 for P(1,3) is 0.52 nm. This represents a percentage difference of 0.596%.

In this table, the smallest percentage of the difference between H1 and H2 for P(1,2) is 0.590%.

Pillar position	P(1,1)	P(1,2)	P(1,3)
X[μm]	2.647	7.617	12.62
Y[μm]	2.441	2.441	2.441
H1[nm]	91.59	94.2	86.65
H2[nm]	92.14	94.76	87.17
D[nm]	0.55	0.56	0.52
D%	0.596%	0.590%	0.596%

Table 2 a comparison of quantitative values of the first row of pillars in the AFM image (Fig.4(a)) with the values of the corresponding row in the restored image (Fig.4(c)).
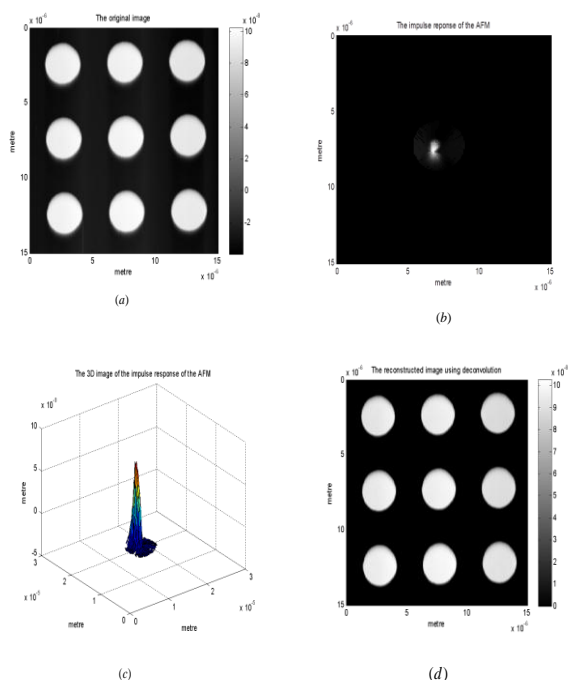
(a)

(b)

(c)

(d)

Fig.4 illustrates a comparison between the raw experimental AFM image and the restored AFM image that was produced using the proposed technique at a scanning speed of 2 Hz: (a) the image of the real sample that contains cylindrical pillars measured by an AFM tip; (b) the 2D view of the impulse response of the AFM; (c) the 3D view of the impulse response of the AFM; (d) the restored AFM image after applying a Lucy-Richardson deconvolution method between the AFM image and the estimated impulse response of the AFM.
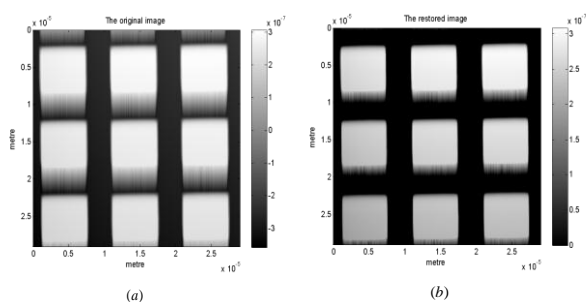

(a)

(b)

Fig.5 illustrates a comparison between the raw experimental AFM image and the restored AFM image that was produced using the proposed technique at a scanning speed of 2 Hz : (a) the image of the real sample that contains square pillars measured by an AFM tip; (b) the restored AFM image after applying a Lucy-Richardson deconvolution method between the AFM image and the estimated AFM impulse response.

3.3 Restoration of AFM images at a scanning speed of 2.5 Hz

Fig.s 6(a), and 7(a) depict the experimental images of a real sample that contains an array of raised cylindrical pillars, and a grid of raised square pillars,

respectively. However, in the following results set these images have been measured by the AFM at a scanning rate of 2.5 Hz.

Restoration of the AFM images of the two real samples can be carried out by applying a Lucy-Richardson deconvolution algorithm between the original AFM image and the impulse response that was derived as explained in section 2 and which is shown in Fig.6(c).The resultant restored AFM images that were produced by applying the deconvolution process are shown in Fig.s 6(d), and 7(b), respectively. As a result of applying the deconvolution algorithm, it can be seen that the quality of the restored AFM images has been qualitatively improved by removing the effects of the convolution by the AFM impulse response that is inherent to the original blurred raw AFM images.

Table 3 shows numerical information from the first raw of pillars in the AFM image that is shown in Fig.6(a) and compared with the numerical information from the corresponding raw in the restored image which is illustrated in Fig.6(d). This AFM image was measured at a scanning speed of 2.5 Hz. The height (H1) of the pillar P(1,1), which is located at (X = 2.647 μm, Y = 2.441 μm) is 93.45 nm. The corresponding height (H2) in the restored image is 94.3 nm. The difference between H1 and H2 for P(1,1) is 0.85 nm, which represents a percentage difference of 0.901%.

For the second pillar in the first row P(1,2), the height (H1) that lies at a position (X = 7.617 μm, Y =2.441 μm) is 91.73 nm, whereas the corresponding height (H2) in the restored image is 92.57 nm. The difference between H1 and H2 is 0.84 nm, which represents a percentage difference of 0.907%.

For the third pillar in the first row P(1,3), the height (H1) is 88.67 nm. The corresponding height (H2) in the restored image is 89.49 nm. The difference (D) between H1 and H2 is 0.82 nm, which corresponds a percentage difference of 0.916%.

From this table, the smallest percentage of the difference between H1 and H2 for P(1,1) is 0.901%.

Pillar position	P(1,1)	P(1,2)	P(1,3)
X[μm]	2.647	7.617	12.62
Y[μm]	2.441	2.441	2.441
H1[nm]	93.45	91.73	88.67
H2[nm]	94.3	92.57	89.49
D[nm]	0.85	0.84	0.82
D%	0.901%	0.907%	0.916%

Table 3 a comparison of quantitative values of the first row of pillars in the AFM image (Fig.6(a)) with the values of the corresponding row in the restored image (Fig.6(d)).
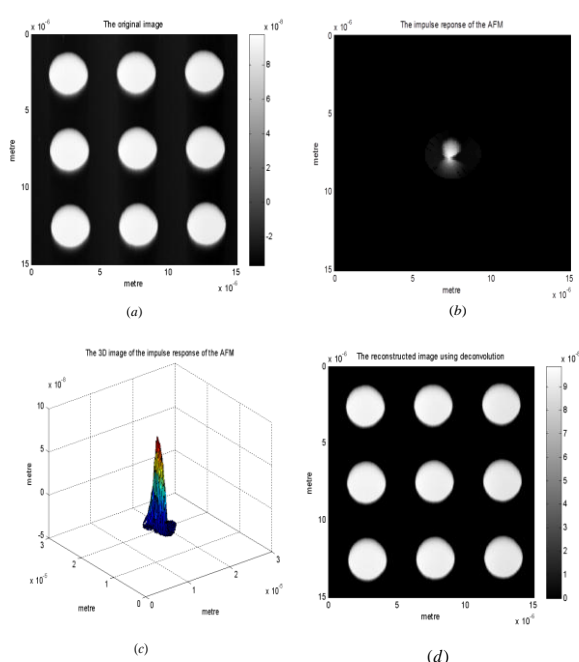

Fig.6 Illustrates a comparison between the raw experimental AFM image and the restored AFM image that was produced using the proposed technique at a scanning speed of 2.5 Hz : (a) the image of the real sample that contains cylindrical pillars measured by an AFM tip; (b) the 2D view of the impulse response of the AFM; (c) the 3D view of the impulse response of the AFM; (d) the restored AFM image after applying a Lucy-Richardson deconvolution method between the AFM image and the estimated impulse response of the AFM.
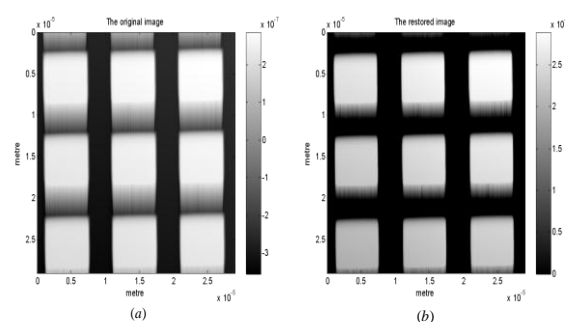

Fig.7 Illustrates a comparison between the raw experimental AFM image and the restored AFM image that was produced using the proposed technique at a scanning speed of 2.5 Hz : (a) The image of the real sample that contains square pillars measured by an AFM tip; (b) The restored AFM image after applying a Lucy-Richardson deconvolution method between the AFM image and the estimated AFM impulse response.

4 Conclusion

In terms of experimental results in this paper, several examples have been introduced. In these examples two different real samples were investigated; a real sample that contains an array of raised cylindrical pillars, and a real sample that contains a grid of raised square pillars. These real samples were measured at three different scanning speeds, namely; 1 Hz, 2 Hz, and 2.5 Hz. Once the AFM impulse response was estimated for each scanning speed, a Lucy-Richardson deconvolution algorithm was performed between the raw AFM images and the impulse response that was derived for that scanning speed. This deconvolution process gave an improvement of results in terms of the fidelity of the measured AFM height images.

Tables 1, 2, and 3 show the quantitative indications of the first row of pillars in the AFM image compared with the corresponding quantitative indications in the restored image at a scanning speeds of 1 Hz, 2 Hz, and 2.5 Hz, respectively. As a result from the quantitative indications, it can be seen that the percentage difference (D) in height between the raw and restored images increases with increasing scanning speeds.

References:

[1] G. S. Pingali and R.Jain, *Restoration of Scanning Probe Microscope Images*, In

Application Of Computer Vision, Palm Springs, CA, USA, 1992.

[2] D. J. Keller and F. S.Franke, "Envelope Reconstruction of Probe Microscope Images," *Surface Science,* P. 11, 1993.

[3] J.S.Villarrubia, Algorithms for Scanned Probe Microscope Image Simulation Surface Reconstruction and Tip Estimation, *Journal of Research of The National Institute of Standards and Technology,* Vol.04, 1997, PP. 425-454.

[4] L.S.Dongmo, J.S. Villarrubia, S.N.Jones, T.B.Renegar, M.T.Postek, and J.F.Song, Experimental Test of Blind Tip Reconstruction for Scanning Probe Microscopy, *Ultramicroscopy,* Vol. 85, 2000, PP. 141 - 153.

[5] T. Brain and E. Steven, A Method to Improve the Quantitative Analysis of SFM Images at the Nanoscale, *Surf. Sci.,* 2001.

[6] D.Tranchida, S.Piccarolo, and R.A.C.Deblieck, Some Experimental Issues of AFM Tip Blind Estimation: The Effect of Noise and Resolution, *Meas. Sci. Technol.,* Vol.17,2006 PP. 2630 – 2636.

[7] L. Lucy, An Iterative Technique for the Rectification of Observed Distributions, *The Astronomical Journal*, Vol. 79, No.6, 1974, pp. 745-754.

[8] W. Richardson, Bayesian-Based Iterative Method of Image Restoration, *J. Opt. Soc. Am.*, Vol. 62, No. 1, 1972, pp. 55-59.

[9] R. Gonzalez, *Digital Image Processing Using Matlab*, Second Edition, Gatemark Publishing, 2009.